RSC Advances

ROYAL SOCIETY OF CHEMISTRY

www.rsc.org/advances

Journal Name

RSCPublishing

ARTICLE

WS_2 nanoadditized lubricant for applications affected by hydrogen embrittlement

Cite this: DOI: 10.1039/x0xx00000x

Vlad Bogdan Niste,[a] Hiroyoshi Tanaka,[b,c] Monica Ratoi[a] and Joichi Sugimura[b,c]

Received ooth January 2012,
Accepted ooth January 2012

DOI: 10.1039/x0xx00000x

www.rsc.org/

Hydrogen is one of the cleanest available vehicle fuels but its small atomic size allows it to diffuse readily through the lattice of solid materials, which can cause catastrophic failure in high strength steels. Metal embrittlement has been identified as a major consequence of hydrogen uptake and represents an extra challenge for lubricated tribological parts in fuel cell vehicles, hydrogen compressors, storage tanks, dispensers and wind turbines that are normally subjected to high stresses. This study has found WS_2 nanoparticles as an effective additive candidate to impede the permeation of hydrogen into rolling element bearings at high temperatures and pressures. Compared to the pure polyalphaolefin (PAO) base oil, WS_2 nanoadditized oil reduced the concentration of permeated hydrogen in the bearing steel and led to controlled wear and smoother tracks. These effects are attributed to the formation of a chemical tribofilm on the wear track which reduces hydrogen embrittlement and extends the life of steel through several mechanisms: 1) its continuous generation impedes formation of nascent catalytic surfaces during rubbing and thus prevents the decomposition of oil/water molecules and generation of atomic hydrogen; 2) acts as a physical barrier to hydrogen permeation through the wear track; 3) the low coefficient of diffusion of hydrogen through the tungsten compounds found in the tribofilm further reduces hydrogen permeation; 4) some of the atomic hydrogen is used up in redox reactions during the formation of the tribofilm and 5) the tribofilm reduces the total amount of water in the steel formed by the reaction of hydrogen atoms with oxides and thus extends the fatigue life. WS_2 nanodditized lubricants can lead to improved profitability and sustainability of the emerging renewable energy industry.

Introduction

Routinely employed in tribological applications and indispensable in moving components subjected to severe conditions, rolling element bearings typically undergo a large number of loading cycles during their lifetime and eventually suffer from a type of surface damage known as rolling contact fatigue (RCF) failure. Recently, operating conditions have become more demanding (higher rotation speed, temperature, vibrations etc.) and in some applications like wind turbine gearboxes and automotive powertrains and peripheral auxiliaries, bearings suffer from a shortening of their service life due to an unusual premature failure damage that differs from the classic RCF described by ISO15243. This consists in the appearance of a peculiar type of white etching areas (WEA) associated with cracks (WEC). WEAs are characterized by two phases: an ultrafine ferrite granular structure several tens of nanometres in diameter [1, 2] with increased hardness (30-50% higher compared to the bulk matrix) and an amorphous-like phase nearing the cracks [3]. WECs are wide discontinuous subsurface three-dimensional network cracks that have their origin at or near the surface (0-150 μm), where the maximum shear stress is located, and propagate towards the core in the over-rolling direction.

The mechanism of the failure mode involving WEC formation is not fully understood, but hydrogen embrittlement and stress concentration are believed to be the most important causes. Proponents of the stress concentration have reported that WECs are formed by the microstructural change caused by the sliding between the ball and the bearing ring (race) and depends on the testing conditions. It was shown that WECs are initiated at the interface between the amorphous and fine granular phases inside WEA and between WEA and the matrix [3]. Researchers who investigated the effect of hydrogen believe that WEAs form as a result of the embrittlement of steel caused by hydrogen. Hydrogen-assisted fatigue reported in fuel cells that use hydrogen as a source of energy was shown to lead to WECs or accelerate classic RCF [4-12]. In atomic form, hydrogen can permeate the metal surface and negatively influence its properties. Metal embrittlement has been identified as a major consequence of the hydrogen uptake and represents an extra challenge for tribological parts in fuel cells that are normally subjected to high stresses.

In hydrogen atmosphere, the RCF life of rolling element bearings was reported to decrease with increasing concentration of hydrogen permeated into the bulk material [13-15]. Higher operating temperatures lead to increased concentrations of hydrogen, which infer that high-temperature operating bearings, as found in wind turbine gearboxes, are more affected. For this reason, some research studies recommend that the lubricant temperature in wind turbine gearboxes is maintained below 75 - 90ºC to reduce hydrogen permeation and extend bearing life.

In applications other than fuel cells, the source of hydrogen is still debated, but the decomposition of water and/or oil molecules catalysed by the fresh metal surface locally generated in severe mixed friction contacts is usually considered responsible [16].

In order to prevent hydrogen permeation several solutions have been proposed. One of them is to generate a protective film on the wear track by employing suitable lubricant additives. Steels are normally covered in a thin oxide film, but this is removed during operation and fresh metal sites are generated.

Previous studies investigated the effectiveness of a range of oils and additives to reduce hydrogen generation and permeation into the steel and to increase the life of the material. The amount of hydrogen generated in vacuum by various types of oils employed to lubricate a ball-on-disc sliding test was found to be proportional to the wear width measured at the end of the test [17] and therefore depends on the lubricity of the oil.

Conventional additives, such as corrosion inhibitors and antiwear/extreme pressure additives that can deactivate the catalytic action of nascent steel surfaces by rapidly forming passivating films or antiwear phosphate and sulphide films, were reported to be efficient at preventing hydrogen generation and permeation in steel to prolong material life [17-20]. The drawback of conventional antiwear additives resides in the fact that film generation usually requires high temperatures and an initial running-in period [17-19]. To overcome this deficiency, particular interest has recently been directed to nanoparticles (NPs), which used as antiwear and extreme pressure oil additives, can easily penetrate the contact due to their nanosize, exfoliate and/or react with the nascent metal surface of the wear track and generate a protecting tribofilm that can prevent both the formation of hydrogen atoms and their permeation into the substrate. From the myriad of potential nanoadditives, boron and molybdenum disulphide (MoS_2) based NPs were shown to generate thick durable tribofilms and smooth tracks and have excellent wear and friction behaviour [21, 22]. These favourable properties could make them promising candidate additives for wind turbine applications [23].

Amongst lubricant nanoadditives, WS_2 NPs have numerous advantageous properties [24-27], but the most important for applications affected by hydrogen embrittlement is their recently discovered ability to react with the steel substrate in high-pressure, high-temperature contacts and form a protective chemical tribofilm. The complex structure and composition of this tribofilm has provided them with an excellent ability to decrease friction in the boundary regime and great antiwear and extreme pressure properties. The former is due to the presence of a top layer of unreacted WS_2 NP sheets, while the latter is explained by the presence of elemental tungsten and tungsten oxide, which enhance its hardness and elastic modulus values [28, 29]. The presence of the complex WS_2 tribofilm has the potential to reduce the permeation of hydrogen in steel and reduce its detrimental effect on the properties of the material.

This study investigates the ability of WS_2 NPs to reduce the concentration of permeated hydrogen in rolling element bearings operating in high temperature and pressure conditions as encountered in bearing gear boxes. Rolling contact tests were conducted using WS_2 additives in polyalphaolefin (PAO) base oil and the concentration of hydrogen in the samples at the end of tests was measured by thermal desorption spectrometry (TDS). The mechanism of action of WS_2 nanoadditives was investigated by performing surface analysis on the rolling tracks using optical profilometry, X-ray photoelectron spectroscopy (XPS) and Auger electron spectroscopy.

Materials and methods

In order to quantify the ability of WS_2 NPs to reduce the permeation of hydrogen into steel and to investigate their basic mechanism of action, no surfactant/dispersant was used to stabilize the dispersion. Alternatively, the test samples were prepared by sonication. The tests were conducted in PAO (polyalphaolefins have low polarity and thus low affinity for steel surfaces) in order to avoid any competition between the WS_2 NPs and the oil molecules for the steel substrate, as discussed in literature [28]. WS_2 dispersions in base oil were prepared at a 0.5 % treat rate. Tests were also performed with pure base oil for comparative reasons. The base oil is a PAO32 with a density of 0.826 g/cm^3 and a viscosity of 28.8 cSt at 40ºC and 5.6 cSt at 100ºC.

The size distribution of the WS_2 NPs dispersed in PAO was recorded immediately after preparation by dynamic light scattering (Malvern ZetaSizer Nano ZS). The intensity distribution showed the presence of two distinct NP population sizes: one with an average diameter of 40 nm and the other of approximately 250 nm [28]. This particular size distribution of NPs can be potentially beneficial to tribological applications, because it increases their ability to penetrate contacts and fill asperity gaps of different sizes, thus limiting the adhesion of contact surfaces and reducing friction.

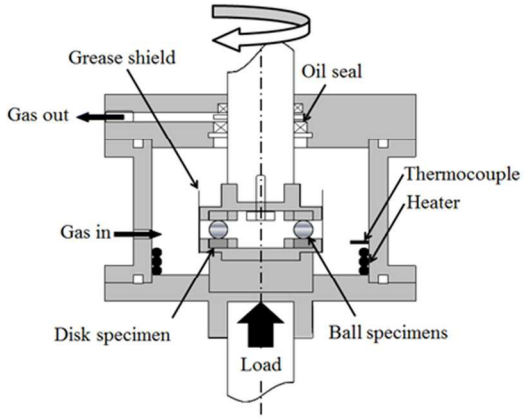

Fig. 1 Diagram of rolling contact test rig

Table 1 Rolling contact test conditions

Test duration	2, 5 and 10 hours
Number of cycles	595,000/h (ball) and 270,000/h (race)
Temperature	120ºC
Load	2650 N
Mean Hertz pressure	4.8 GPa
Entrainment speed	1500 rpm (3.4 m/s)
Film parameter Λ	2

Tribological tests were performed in a ball-on-disc setup test rig. Figure 1 shows a schematic illustration of the apparatus. Six 6.35 mm diameter balls are placed on a guide disc with raceway grooves and separated by a retainer. Normal load (2650 N equivalent to a Hertz pressure of 4.8 GPa) is applied to the chamber by a lever and the disc/ball contact undergoes rolling through the rotation of the upper shaft. The contact pressure used in this study is higher than the calculated pressure encountered during normal operation in bearings, in order to accelerate the formation of hydrogen and initiation of embrittlement and is in line with recommendations from other publications [4, 10, 15, 14, 30]. The Hertzian pressure is slightly higher than the shakedown limit (the maximum contact pressure which the material can support in the elastic range in steady state conditions). Theoretically this means that plastic deformation below the surface continues to occur repeatedly. In practice however, the pressure reduces due to the change in surface geometry (to become more conformal) by initial deformation and wear, and virtually elastic contact occurs in the rest of the cycles. The Hertzian contact pressure for the dynamic load rating (load for a rating life of 10^8 load cycles) of this steel is 4.2 GPa. The ball and disc steel is JIS SUJ2, equivalent to AISI 52100. The disc specimens were polished with sandpaper followed by buff polishing with 3-µm diamond slurry to an Ra (arithmetic average roughness) of 0.05 µm. The Ra indicates the degree of deviation from the mean value. The contact is subjected to mixed lubrication conditions. The specimens were ultrasonically cleaned with hexane and acetone prior to the rolling contact tests. Table 1 summarizes the testing conditions.

The hydrogen content in the steel samples was measured using TDS (Denshi-Kagaku TDS1200). The technique consists of heating the sample under a constant temperature gradient in order to induce the desorption of all gaseous species, which are than analysed by a mass spectrometer. Immediately after the rolling contact tests, the specimens were cooled, cleaned in an ultrasonic bath with hexane and acetone and small pieces (7x3.5x1 mm, weighting approximately 0.2 g) were cut from the rolling contact area. During the TDS analysis, the cut disc and ball pieces were heated from room temperature to 800ºC at a rate of 60ºC/min and 10ºC/min respectively, which leads to the desorption of all gaseous species from the test samples. A lower rate of heating was used for the ball due to its larger mass and subsequent thermal inertia. The TDS rig is equipped with a quadrupole mass spectrometer that can measure and analyse the hydrogen species released from the disc and ball specimens.

Optical profilometry (Bruker ContourGT) was used to investigate the depth and morphology of the wear tracks on the disc specimens after each test. The equipment generates a 3D surface profile of the wear track that can be analysed with the supplied software. For each image multiple surface profiles were measured and used to calculate average depth values.

XPS combined with Argon ion sputtering for depth profile analysis (JEOL JPS 9200 X-ray Microprobe) was used to measure the composition, chemical state and electronic state of the samples, and was performed on the tribofilms at the end of the tests. The excitation source was a monochromatized Al Ka (1476.6 eV) X-ray beam of 100 µm diameter. The instrument spectral resolution was 1.1 eV (path energy). Points *on* and *off* the wear track were selected by optical micrograph imaging. In depth profiling experiments were alternated with rastered Ar^+ beam milling. The milling rate was calibrated using a SiO_2/Si substrate with known oxide thickness, in accordance with standard techniques. Sputtering was performed for 30 seconds, equivalent to an estimated depth of 2 nm.

An Auger electron spectrometer (JEOL JAMP 9500 F) with 10 keV electron beam was used to investigate the elemental distribution across the wear track. Ion sputtering was also performed before the analysis in order to remove the contaminated layer on the surface for 10 seconds, equivalent to an estimated depth of 3 nm.

Results and discussion

Tribological tests employing WS_2 NP oil dispersions and the PAO base oil were performed in the conditions described in Table 1. To compare the different lubricants, the total amount of hydrogen released from the specimens during heating was measured using TDS, which monitors the rate of hydrogen release from samples by an applied temperature ramp.

In the high-stress, high-temperature conditions encountered in systems for supplying hydrogen such as compressors, both hydrogen gas and oil molecules can decompose on the fresh metal sites generated on the wear track and create atomic hydrogen [30]. The passage of the hydrogen atoms through steel is hindered by lattice imperfections that tend to attract and bind them, thus rendering atoms immobile at temperatures where they should be able to diffuse readily. This phenomenon is known as 'trapping'. The hydrogen atoms that permeate the steel substrate can be trapped in the bulk material or/and at grain boundary interfaces, or they can be confined by their chemical reaction with other atoms (e. g. oxygen atoms from oxide particles). During the TDS analysis, the hydrogen desorption process must be proceeded by the breakage of the physical/chemical bonds formed by the hydrogen atoms inside the specimen. The bonding energy between hydrogen and different atoms varies, and therefore, as the sample is heated during the desorption process, the mass spectrometer records complex signals. Furthermore, as hydrogen desorbs from the steel sample, it can combine with other gas atoms (especially oxygen) to generate hydrogen-containing species (most commonly water). When quantifying the hydrogen permeation into the substrate, all hydrogen containing species must be taken into account [31].

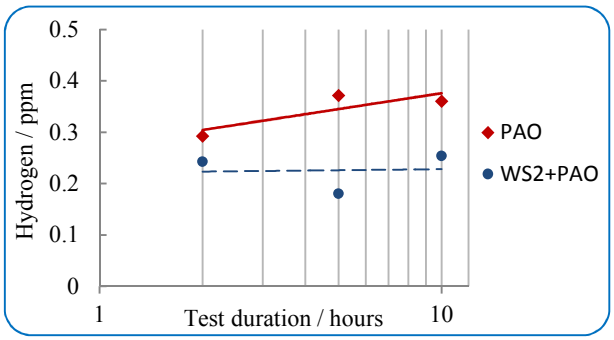

Fig. 2 Concentration of hydrogen in the disc specimens after 2, 5 and 10 h of lubrication with WS_2 additized and non-additized PAO oil

As shown in Figure 2, the total amount of hydrogen (in ppm) permeated in the disc specimen was reduced by approximately 30% when lubrication was carried out with WS_2-additized PAO as compared to the PAO oil. These values were obtained by integrating the desorption spectra recorded during the TDS analysis and are corrected for the mass of each specimen. The signals recorded for the disc and ball samples

have a similar profile and therefore, only analysis performed on the disc samples is shown.

Figure 3 shows the desorption curve for hydrogen (m/z=2) and water (m/z=18) from samples lubricated with the PAO base oil. Other hydrogen containing species were also monitored but their concentration was very low. The small discrepancies in the position and size of peaks may be due to the difference between the real temperature of the specimens and the temperature determined by the thermocouple, the small variations in the thermal capacity of the samples or any surface films formed on the wear tracks. The similar intensity of the signal at 200ºC after 5 and 10 hours may be an indication of diffusion after prolonged rolling.

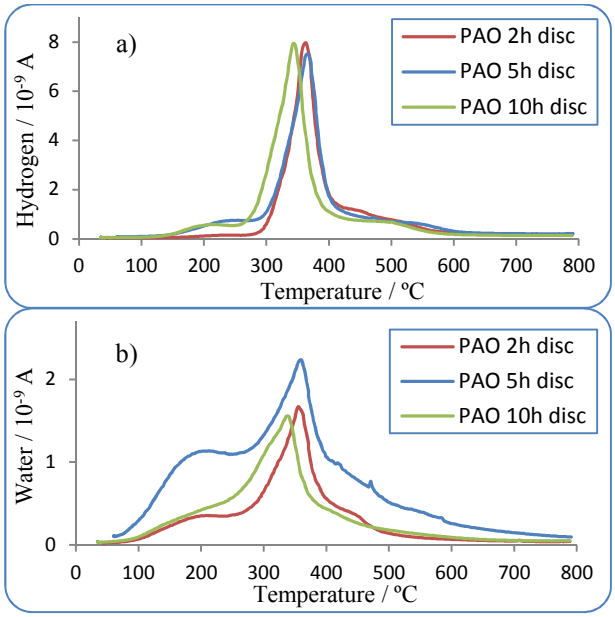

Fig. 3 Desorption spectra of hydrogen (a) and water (b) from the samples tested with PAO

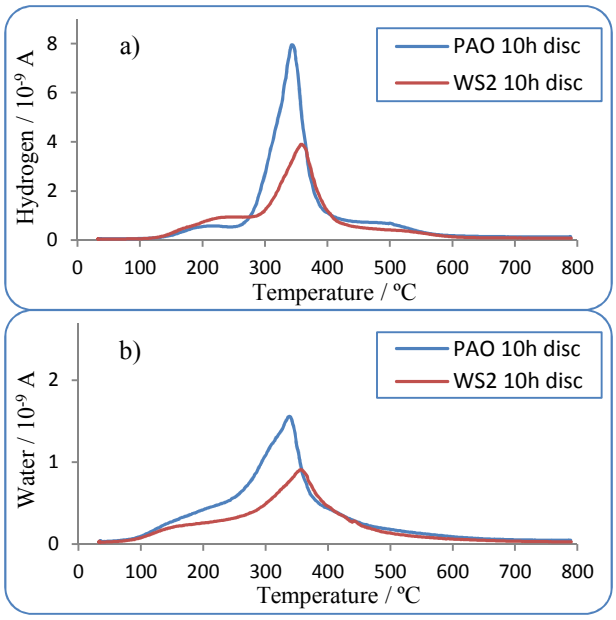

Fig. 4 Desorption spectra of hydrogen (a) and water (b) for PAO and PAO+WS_2 samples

Previous research shows that the position of the desorption peaks depends on the tribological testing conditions (material properties, temperature) and TDS analysis heating rate [32-36].

In this study, the first hydrogen peak is at around 150-200ºC (Figure 3a) and is attributed to atoms trapped at the interface with metal oxide particles, although previous research does not explain the nature of the bonds [37, 38]. The concentration of these species increases with the length of the experiment. This can be explained by the accumulation of larger amounts of hydrogen atoms in the sample, which are then more likely to react with the oxide species in the material.

The peak at 350-400ºC corresponds to hydrogen atoms trapped in the bulk material, at dislocations, microvoids and grain boundary interfaces, and is the main signal recorded during the analysis [32-34, 39-41]. The hydrogen bound to undissolved metal carbides and highly disorientated grain boundary interfaces has higher binding energies and is therefore released at very high temperatures (the signal above 400ºC) [32-33, 39-41].

Apart from hydrogen, water desorption kinetics were also measured using the TDS apparatus (Figure 3b). As observed from the spectra, water can be adsorbed at the surface and then desorbed when the sample is heated (the signal occurring at 100ºC). There are also additional peaks, corresponding to hydrogen trapped in the steel, which has reacted with oxygen to form water molecules during the desorption process from the material (signals at ~200ºC and ~350ºC). The sources for this hydrogen can be from metal oxide grain boundaries, as well as hydrogen atoms trapped in the bulk material. Hydrogen trapped at the interface with oxide species is more likely to form water molecules and therefore in this case, the intensity of the signal at ~200ºC is relatively higher compared to the signal at ~350ºC corresponding to the bulk hydrogen.

Figure 4a compares the hydrogen signals from the tests lubricated with PAO and PAO+WS_2 for 10 hours. The shape of the curves is similar, but the amount of hydrogen bound to metal oxide species (the signal at 150-200ºC) is larger for the WS_2 sample. These results are compatible with previous findings, which showed that WS_2 NPs react with the wear track and generate a tribofilm rich in metal oxides. The metal oxides interact with hydrogen atoms and trap them at the interface.

Figure 4b shows the water desorption spectra of the disc samples for both lubricants. The results reveal that WS_2 reduces the amount of water in the substrate, compared to the base oil.

The amount of water detected consists of the molecules adsorbed on the surface and/or inside the steel substrate, and water formed from the reaction of hydrogen atoms with oxides. The presence of water in the substrate is detrimental to the life of the steel, as it can initiate oxidation in the substrate, interact with the scale interior to affect its microstructure and properties [42] and promote the growth of any cracks present in the material [43]. By reducing the water content through tribofilm generation, WS_2 additives can exert a beneficial effect on the lubricated steels.

To investigate why the WS_2-additized PAO significantly reduced the total amount of hydrogen permeated in the disc specimen (by 30%) as compared to the PAO oil, the wear tracks were physically and chemically characterized. 3D profilometry images of the wear tracks at the end of the tests (2, 5 and 10 hours) and the corresponding track profiles are shown in Figure 5. In all tests, the WS_2 lubricant generated slightly wider, but smoother tracks than the base oil.

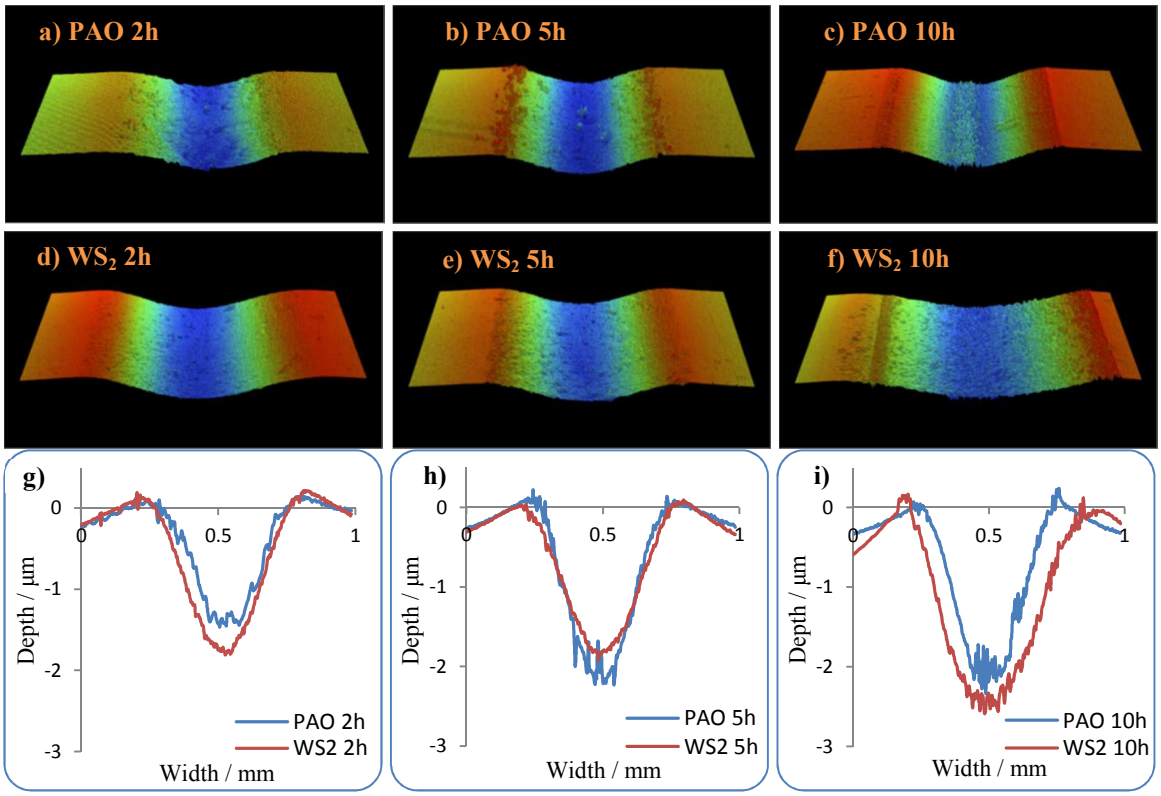

Fig. 5 Profilometry images (a) – (f) and wear track profiles (g) – (i) for pure PAO and PAO + WS_2

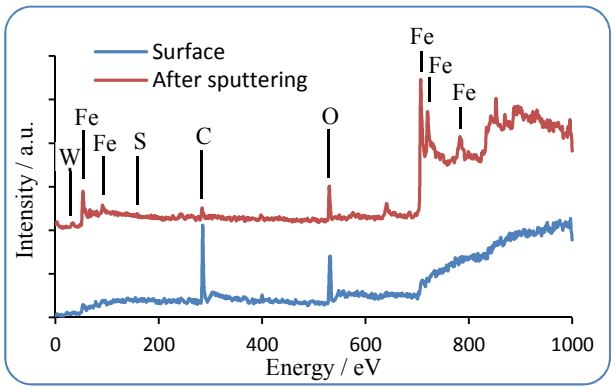

Fig. 6 XPS spectra for the PAO+WS_2 10h lubricated specimen, before and after ion sputtering

As reported in numerous publications, during testing involving high loads the edges of the wear track become slightly raised. The height of the side ridges or furrows due to plastic deformation of the track may not change unless there are additional piles due to wear. This situation was seen in an almost similar degree in all our tests shown in Fig. 5 (a) – (f).

Chemical analysis (XPS) was performed on the wear tracks in order to investigate the presence of a tribofilm generated during the 10 hour tests and to measure the elemental composition and chemical state of elements in the tribofilm. Figure 6 shows the wide spectra for the WS_2-additized lubricant, recorded at the surface of the wear track and after sputtering of the top contamination layer. At the surface, only carbon and oxygen were detected (from the degradation of the oil). Below the surface layer, the tribofilm contains mainly iron, oxygen and tungsten. Sulphur only gave a very weak signal, while the other small signals are given by the other constituents of the steel substrate.

XPS was also performed on the pure PAO sample tested for 10 h. The comparative core level spectra for Fe 2p and W 4f of the wear tracks lubricated with WS_2-additized and pure PAO lubricants are shown in Figure 7.

The XPS analysis was performed after sputtering of the top 2 nm (30 s) to remove impurities and carbon species from decomposed oil molecules. For the PAO lubricated specimen, iron is found mostly in its oxide form. The wear track of the PAO+WS_2 lubricated sample exhibited main signals for tungsten in the form of W^0 (31.4 eV) and W^{6+} (35.6 eV, specific for WO_3) and iron in both oxide (708.9 eV) and elemental state (706.6 eV). The rest of the signals recorded are attributed to sulphur (S_{2p}, 162 eV), carbon (C_{1s}, 285 eV), oxygen (O_{1s}, 530 eV), iron (Fe_{3p}, 53 eV; Fe_{3s}, 92 eV; Fe_{2p}, 707 and 720 eV; Fe_{LMM}, 784 eV; Fe_{2s}, 845 eV) and other elements present in the steel: manganese (Mn_{2p}, 641 eV; Mn_{LMM}, 852 and 900 eV), nickel (Ni_{2p}, 853 and 870 eV) and copper (Cu_{2p}, 933 eV). The values have been verified against literature data [44]. These findings are in agreement with previous reported results [28] and indicate a reaction between the WS_2 nanoadditive and the steel wear track, with the formation of iron sulphides, tungsten trioxide and elemental iron and tungsten. This type of chemical reaction that generates a tribofilm is characteristic of antiwear additives and explains the morphology of the wear tracks showing wider and smoother profiles. The XPS analysis of C_{1s} also revealed a small amount of carbides present on the tribofilm, which may also help increase the mechanical properties of the tribofilm.

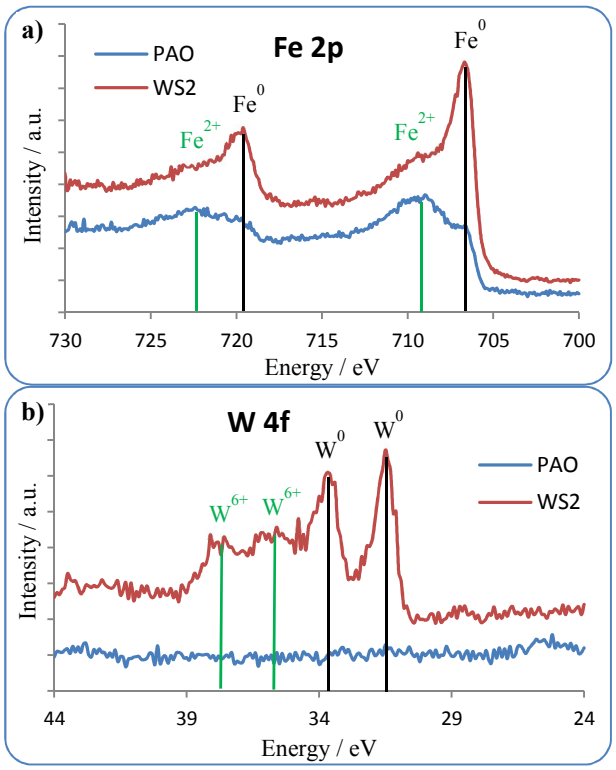

Fig. 7 XPS spectra of Fe 2p and W 4f for the PAO 10h and PAO+WS_2 10h lubricated specimens

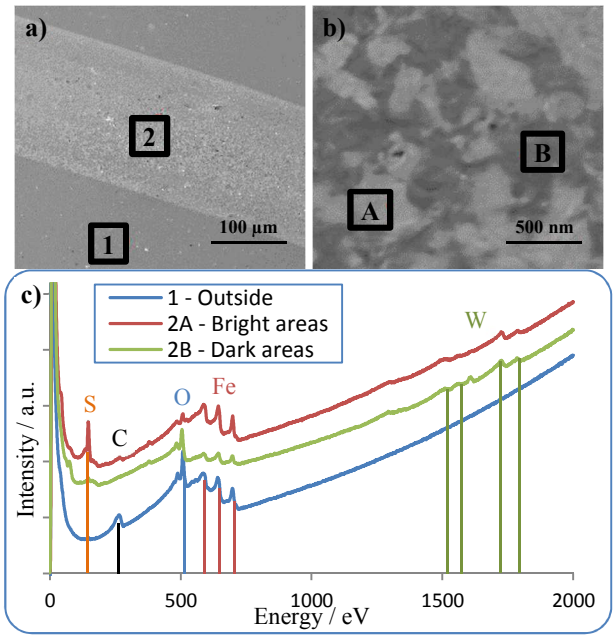

Fig. 8 (a, b) Secondary electron images of the wear track and location of the Auger analysis on the PAO + WS_2 10h lubricated specimen and (c) Auger spectra showing the chemical composition in (2A and 2B) and out (1) of the wear track

To achieve a better understanding of the mechanism of the NP reaction with the steel substrate, the wear track of the 10-hour WS_2 lubricated specimen was subjected to further analysis employing Auger spectroscopy.

Figure 8 shows the location of the analysis and the corresponding Auger spectra. Outside the wear track (position 1), only carbon (from decomposed oil), oxygen and iron were detected. Inside the track (position 2), two separate regions were found with SEM imaging, bright (A) and dark (B), and chemical analysis was performed on each of these sections. The spectra indicate that the bright regions (A) are rich in iron and sulphur compounds, but also contain some amounts of tungsten species. The dark regions display mostly oxygen and tungsten species and small amounts of iron. The results indicate the predominant presence of iron sulphides in the bright areas and tungsten oxides in the dark areas. The signals identified were carbon (C_{KLL}, 269 eV), oxygen (O_{KLL}, 509 eV), iron (Fe_{LMM}, 592 eV, 645 eV and 700 eV), sulphur (S_{LMM}, 148 eV) and tungsten (W_{MNN}, 1512 eV, 1565 eV, 1726 eV and 1787 eV). The values have been verified against literature data [45].

Auger elemental mapping was performed on the wear track of the WS_2-lubricated specimen to visualize the distribution of the main constituents of the tribofilm. As seen in Figure 9, the distributions of iron and sulphur are similar and indicate the presence of iron sulphides. The rest of the investigated area is covered by oxygen compounds. Tungsten is found more uniformly distributed across the track, as also seen in the Auger spectra recorded in both dark and bright areas.

The results of the XPS and Auger analysis are in good agreement and indicate the generation of a thin tribofilm on the wear track. The formation of the chemical film can explain the controlled wear seen during the testing (2, 5 and 10 hours) and the smoother wear tracks produced by the WS_2 lubricant. The properties of the tribofilm reported in previous studies account for the reduced hydrogen permeated in the bearing steel.

These effects are achieved through a number of mechanisms. The continuous generation of film through the reaction of WS_2 with the wear track impedes the formation of fresh, catalytic surfaces during rubbing and thus prevents the decomposition of oil/water molecules and generation of atomic hydrogen.

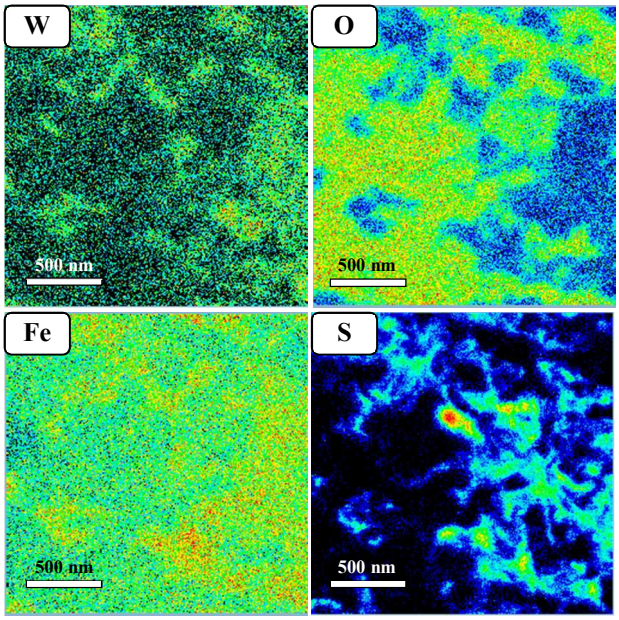

Fig. 9 Auger elemental mapping for the PAO+WS_2 specimen

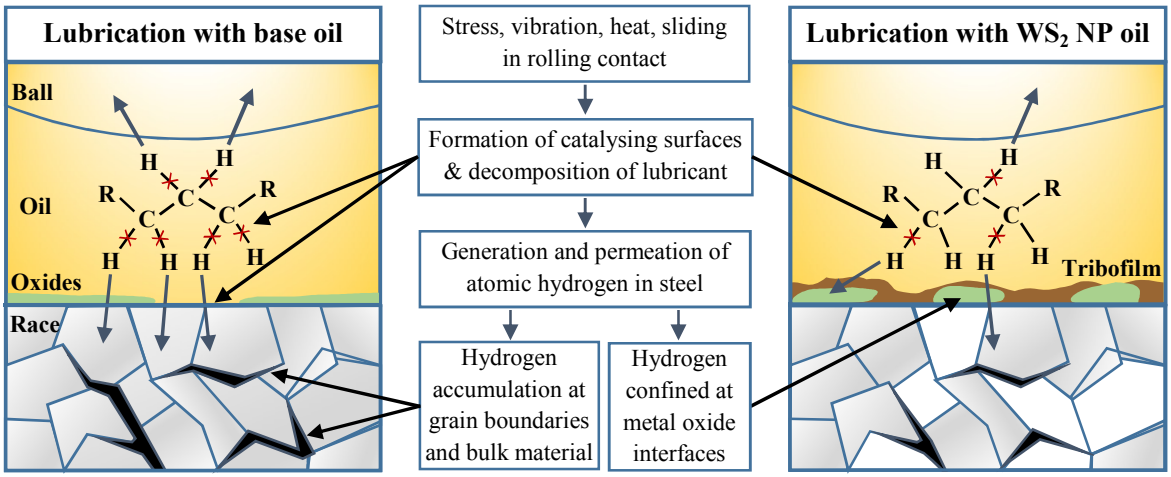

Fig. 10 Schematic showing a comparison between the mechanism of PAO and WS_2-additized PAO to reduce hydrogen embrittlement. For simplification, only embrittlement of the race is shown.

The tribofilm can also act as a physical barrier for hydrogen permeating through the wear track. Previous research showed that a thin layer of nickel electrodeposited on the steel substrate can effectively reduce hydrogen permeation due to its very small coefficient of hydrogen diffusion as compared to the coefficient of diffusion through steel [30]. It was also reported that the diffusion coefficient of hydrogen through steel decreases with the increase of tungsten content [46].

Therefore, the chemical composition of the WS_2 generated tribofilm, comprising of tungsten in elemental and oxide form, could be an effective obstacle to the permeation of hydrogen atoms in steel.

The presence of tungsten in the tribofilm also increases its hardness and results in less wear. This delays the formation of active catalytic surfaces on the metal substrate and prevents the generation of atomic hydrogen.

Furthermore, hydrogen may play an active role in the generation of the tribofilm – tungsten and iron are also found in their elemental states in the film and some amounts of hydrogen could be used up for the chemical reduction of these metal species to their elemental form instead of permeating the steel.

All the up mentioned discussed benefits offered by the WS_2 additized oil in reducing hydrogen embrittlement have been summarized in Figure 10.

Previous studies of the WS_2 nanoadditive, which employed milder loading conditions (1 GPa), resulted in a tribofilm formed only on the wear track, above the surface level. The thickness of the tribofilm could be measured with optical interferometry (SLIM) and profilometry (Alicona) and it was found to be of approx. 100 nm. The tribofilm showed a uniform chemical composition across the track and had a layered structure. The upper part was composed of unreacted WS_2 sheets and/or squashed WS_2 NPs, WO_3, iron oxides and sulphides, while the deeper layers and the interface with the steel substrate consisted of WO_3 and elemental tungsten and iron [28, 29].

The severe contact conditions employed in the current study, with contact pressures of 4.8 GPa specifically used to accelerate the wear process, generated wear scars below the surface level which did not allow the measurement of the tribofilm thickness. Figures 8b and 9 show the presence of a tribofilm and its chemical composition varies across the scanned area. The elemental mapping of the tribofilm revealed the presence of two chemically different regions. This indicates that the tribofilm is either partly formed or partly worn off. In a tribological contact, the film growth is controlled by its generation (chemical reaction kinetics) and removal (wear) rates, which depend on the operating conditions, such as temperature, time, load, slide-roll ratio etc. [47-49]. In practical applications the contact pressures in bearings are much lower than those used in this study, which favours the generation of thicker and more uniform films. These properties of the tribofilm have the potential to increase their efficiency to impede permeation of hydrogen into bearing steel.

Conclusions

In previous studies we have reported that WS_2 NPs react with the steel substrate at high temperatures and pressures to form a protective tribofilm. This study has investigated the ability of this tribofilm to reduce the permeation of hydrogen into rolling element bearings and thus prevent hydrogen embrittlement.

Rolling contact tests were conducted in a ball-on-disc setup using WS_2-additized and plain PAO oil as lubricants. The concentration of hydrogen in the specimens, measured with TDS at the end of the tests, was significantly reduced for the WS_2-additized oil. The results were attributed to the chemical tribofilm generated on the wear track during the test and its specific properties.

Chemical analysis performed on the WS_2 tribofilm revealed the presence of two different regions: one rich in iron sulphides, while the other is mostly composed of tungsten trioxide. This composition suggests an intermediary state during the formation of a full chemical tribofilm.

The tribofilm accounts for the controlled wear recorded during the testing (2, 5 and 10 hours), smoother wear tracks and the reduced hydrogen concentration permeated in the bearing steel. These effects are achieved through: 1) the continuous generation of film through the reaction of WS_2 with the wear track, which impedes the formation of fresh, catalytic surfaces during rubbing and thus prevents the decomposition of oil/water molecules and generation of atomic hydrogen; 2) acting as a physical barrier for hydrogen permeation through the wear track; 3) the lower coefficients of hydrogen diffusion in tungsten compounds, which impede hydrogen permeation; 4)

the contribution of hydrogen to the generation of the tribofilm by redox reactions (i.e. reducing the chemical state of tungsten and iron).

WS_2 tribofilms reduce the total amount of water in the steel, entailing both surface and bulk-adsorbed molecules and water formed from the reaction of hydrogen atoms with oxides. By reducing the water content, WS_2 additives can exert a beneficial effect on lubricated steels, such as extending the life of the steel, inhibiting oxidation in the substrate and decelerating the growth of any cracks present in the material.

The results of the study indicate that WS_2 nanoadditives can reduce hydrogen embrittlement of bearing steel and extend RCF life. WS_2 NPs are a promising candidate for applications affected by hydrogen embrittlement, but further work must be carried out to determine optimal operating conditions.

Acknowledgements

The authors wish to acknowledge the Japanese Society for the Promotion of Science for sponsoring this study in the form of an International Research Fellowship.

Notes and references

[a] Faculty of Engineering and Environment, University of Southampton, Highfield Campus, Southampton SO17 1BJ, United Kingdom
[b] Research Center for Hydrogen Industrial Use and Storage, Kyushu University, 744 Motooka, Nishi-ku, Fukuoka 819-0395, Japan
[c] International Institute for Carbon-Neutral Energy Research, Kyushu University, 744 Motooka, Nishi-ku, Fukuoka 819-0395, Japan

1 M. Shibata, M. Goto, N. Oguma, T. Mikami, A new type of micro-structural change due to rolling contact fatigue on bearings for the engine auxiliary devices, *Proc. Int. Tribol. Conf.*, 1995, **3**, 1351.
2 N. Mitamura, H. Hidaka, S. Takaki, Microstructural development in bearing steel during rolling contact fatigue, *Mater. Sci. Forum*, 2007, **539-543**, 4255-4260.
3 H. Harada, T. Mikami, M. Shibata, D. Sokai, A. Yamamoto, H. Tsubakino, Microstructural changes and crack initiation with white etching area formation under rolling/sliding contact in bearing steel, *ISIJ Int.*, 2005, **45**(12), 1897-1902.
4 J. A. Ciruna, H. J. Szeileit, The effect of hydrogen on the rolling contact fatigue life of AISI 52100 and 440C steel balls, *Wear*, 1973, **24**, 107-118.
5 H. K. Birnbaum, P. Sofronis, Hydrogen-enhanced localized plasticity-a mechanism for hydrogen-related fracture, *Mater. Sci. Eng.*, 1994, **A176**, 191-202.
6 A. Grabulov, Fundamentals of rolling contact fatigue, PhD Thesis, University of Belgrade, 2010.
7 M.-H. Evans, A. D. Richardson, L. Wang, R. J. K. Wood, Effect of hydrogen on butterfly and white etching crack (WEC) formation under rolling contact fatigue (RCF), *Wear*, 2013, **306**(1-2), 226-241.
8 K. Stadler, A Stubenrauch, Premature bearing failure in industrial gearboxes, *Antriebstechnisches Kolloquium (ATK)*, 2013, Aachen, Germany.
9 A. Ruellan, F. Ville, X. Kleber, A. Arnaudon, D. Girodin, Understanding white etching cracks in rolling element bearings: The effect of hydrogen charging on the formation mechanisms, *Proc. Inst. Mech. Eng., Part J*, 2014, **228**(11), 1252-1265.
10 H. Uyama, H. Yamada, H. Hidaka, N. Mitamura, The effects of hydrogen on microstructural change and surface originated flaking in rolling contact fatigue, *Tribology Online*, 2011, **6**(2), 123-132.
11 H. Uyama, H. Yamada, White structure flaking in rolling bearings for wind turbine gearboxes, *Wind systems*, 2014. http://www.windsystemsmag.com/article/detail/619/white-structure-flaking-in-rolling-bearings-for-wind-turbine-gearboxes Retrieved: October 2014.
12 H. Hamada, Y. Matsubara, The influence of hydrogen on tension-compression and rolling contact fatigue properties of bearing steel, *NTN Technical Review*, 2006, **74**, 54-61.
13 H. Tanaka, M. Hashimoto, J. Sugimura, Y. Yamamoto, Rolling contact fatigue of bearing steel in hydrogen environment, *World Tribology Congress III*, 2005, **1**, 155-156.
14 T. Otsu, H. Tanaka, K. Ohnishi, J. Sugimura, Simple experiment on permeation of hydrogen into steel in cyclic contact, *Tribology Online*, 2011, **6**(7), 311-316.
15 H. Tanaka, T. Morofuji, K. Enami, M. Hashimoto, J. Sugimura, Effect of environmental gas on surface initiated rolling contact fatigue, *Tribology Online*, 2013, **8**(1), 90-96.
16 L. Grunberg, D. T. Jamieson, D. Scott, Hydrogen penetration in water-accelerated fatigue of rolling surfaces, *Philos. Mag.*, 1963, **8**(93) , 1553-1568.
17 M. Kohara, T. Kawamura, M. Egami, Study on mechanism of hydrogen generation from lubricants, *Tribol. Trans.*, 2006, **49**(1), 53-60.
18 T. Endo, D. Dong, Y. Imai, Y. Yamamoto, Study on rolling contact fatigue in hydrogen atmosphere – Improvement of rolling contact fatigue life by formation of surface film, Life Cycle Tribology, *Tribol. Interface Eng. Ser.*, 2005, Ed. Dowson et al., Elsevier B.V., **48**, 343-350.
19 R. Lu, H. Nanao, K. Kobayashi, T. Kubo, S. Mori, Effect of lubricant additives on tribochemical decomposition of hydrocarbon oil on nascent steel surfaces, *J. Jpn. Pet. Inst.*, 2010, **53**(1), 55-60.
20 C. Newlands, A. Olver, N. Brandon, Gaseous evolution of hydrogen from hydrocarbon oil and grease lubricated contacts, *Tribol. Ser.*, 2003, **41**, 719-726.
21 A. Verma, W. Jiang, H. H. Abu Safe, W. D. Brown, A. P. Malshe, Tribological behavior of deagglomerated active inorganic nanoparticles for advanced lubrication, *Tribol. Trans.*, 2008, **51**(5), 673-678.
22 A. Erdemir, Boron-based solid nanolubricants and lubrication additives, In Nanolubricants, 2008, ed. J. M. Martin and N. Ohmae, John Wiley & Sons Ltd UK, 203-223.
23 R. Errichello, S. Sheng, J. Keller, A. Greco, Wind turbine tribology seminar- A recap, 2011. www.nrel.gov/docs/fy12osti/53754.pdf Retrieved: October 2014.
24 F. Abate, V. D'Agostino, R. Di Giuda, A. Senatore, Tribological behaviour of MoS2 and inorganic fullerene-like WS2 nanoparticles under boundary and mixed lubrication regimes, *Tribology*, 2010, **4**(2), 91–98.
25 L. Rapoport, V. Leshchinsky, I. Lapsker, Yu. Volovik, O. Nepomnyashchy, M. Lvovsky, R. Popovitz-Biro, Y. Feldman, R. Tenne, Tribological properties of WS2 nanoparticles under mixed lubrication, *Wear*, 2003, **255**(7), 785–793.

26 L. Joly-Pottuz, F. Dassenoy, M. Belin, B. Vacher, J. M. Martin, N. Fleischer, Ultralow-friction and wear properties of IF-WS2 under boundary lubrication, *Tribol. Lett.*, 2005, **18**(4), 477–484.
27 J. M. Martin, N. Ohmae, Nanoparticles made of metal dichalcogenides, in *Nanolubricants; Volume 13 of Tribology in Practice Series*, John Wiley & Sons, Chichester, 2008, 15–40.
28 M. Ratoi, V. B. Niste, J. Walker, J. Zekonyte, Mechanism of action of WS2 lubricant nanoadditives in high-pressure contacts, *Tribol. Lett.*, 2013, **52**(1), 81–91.
29 M. Ratoi, V. B. Niste, J. Zekonyte, WS2 nanoparticles – potential replacement for ZDDP and friction modifier additives, *RSC Adv.*, 2014, **4**(41), 21238-21245.
30 N. Kino, K. Otani, The influence of hydrogen on rolling contact fatigue life and its improvement, *JSAE Rev.*, 2003, **24**, 289-294.
31 H. Tanimoto, H. Tanaka, J. Sugimura, Observation of hydrogen permeation into fresh bearing steel surface by thermal desorption spectroscopy, *Tribology Online*, 2011, **6**(7), 291-296.
32 B. A. Szost, R. H. Vegter, P. E. J. Rivera-Diaz-del-Castillo, Hydrogen trapping mechanisms in nanostructured steels, *Metall. Mater. Trans. A*, 2013, **44**(10), 4542-4550.
33 F. G. Wei, T. Hara, K. Tsuzaki, Precise determination of the activation energy for desorption of hydrogen in two Ti-added steels by a single thermal-desorption spectrum, *Metall. Mater. Trans. B*, 2004, **35**(3), 587-597.
34 Joo Hyun Ryu, Hydrogen embrittlement in TRIP and TWIP steels, PhD Thesis, Pohang University of Science and Technology, 2012.
35 D. Perez Escobar, E. Wallaert, L. Duprez, A. Atrens, K. Verbeken, Thermal desorption spectroscopy study of the interaction of hydrogen with TiC precipitates, *Met. Mater. Int.*, 2013, **19**(4), 741-748.
36 S. Frappart, A. Oudriss, X. Feaugas, J. Creus, J. Bouhattate, F. Thebault, L. Delattre, H. Marchebois, Hydrogen trapping in martensitic steel investigated using electrochemical permeation and thermal desorption spectroscopy, *Scr. Mater.*, 2011, **65**, 859-862.
37 A. Yamauchi, Y. Yamauchi, Y. Hirohata, T. Hino, K. Kurokawa, TDS measurement of hydrogen released from stainless steel oxidized in H_2O-containing atmospheres, *Mater Sci. Forum*, 2006, **522**(523), 163-170.
38 L. Begrambekov, O. Dvoychenkova, A. Evsin, A. Kaplevsky, Ya. Sadovskiy, N. Schitov, S. Vergasov, D. Yurkov, Hydrogen transport through metal oxide surface under atom and ion irradiation, *J. Phys.: Conf. Ser.*, 2014, **567**, 012003.
39 J. P. Hirth, Effects of hydrogen on the properties of iron and steel, *Metall. Trans. A*, 1980, **11**(6), 861-890.
40 A. H. M. Krom, A. D. Bakker, Hydrogen trapping models in steel, *Metall. Mater. Trans. B*, 2000, **31**(6), 1475-1482.
41 J. R. Scully, H. Dogan, D. Li, R. Gangloff, Controlling hydrogen embrittlement in ultra-high strength steels, Corrosion 2004, New Orleans, March 2004.
42 D. J. Young, Effects of water vapour on oxidation, In *High Temperature Oxidation and Corrosion of Metals*, Elsevier, 2008, 455-496.
43 M. Kamaya, Environmental effect on fatigue strength of stainless steel in PWR primary water – Role of crack growth acceleration in fatigue life reduction, *Int. J. Fatigue*, 2013, **55**, 102-111.
44 J. F. Moulder, W. F. Stickle, P. E. Sobol, K. D. Bomben, Handbook of X-ray Photoelectron Spectroscopy: A Reference Book of Standard Spectra for Identification and Interpretation of XPS Data, Physical Electronics Inc, 1995.
45 L. E. Davis, N. C. MacDonald, P. W. Palmberg, G. E. Riach, R. E. Weber, Handbook of Auger Electron Spectroscopy: A Reference Book of Standard Data for Identification and Interpretation of Auger Electron Spectroscopy Data, Physical Electronics Division, 1976.
46 J. K. Wu, C. W. Su, Hydrogen permeability and diffusivity in low tungsten steels, *J. Mater. Sci. Lett.*, 1988, **7**, 347-349.
47 M. Ratoi, V. B. Niste, H. Alghawel, A. Suen, K. Nelson, The Impact of Organic Friction Modifiers on Engine Oil Tribofilms, *RSC Adv.*, 2014, **4**, 4278-4285.
48 J. M. Palacios, Thickness and chemical composition of films formed by antimony dithiocarbamate and zinc dithiophosphate, *Tribol. Int.*, 1986, **19**(1), 35-39.
49 J. M. Palacios, Films formed by antiwear additives and their incidence in wear and scuffing, *Wear*, 1987, **114**(1), 41-49.